BROOKHAVEN NATIONAL LABORATORY

BNL-79632-2007-CP

Calibration and Testing of a Large-Area Fast-Neutron Directional Detector

Peter E. Vanier, *Member, IEEE*, Leon Forman, Istvan Dioszegi, Cynthia Salwen, and Vinita J. Ghosh

Brookhaven National Laboratory, Upton, NY 11973

Nonproliferation and National Security Department
Detector Development and Testing Division

Brookhaven National Laboratory
P.O. Box 5000
Upton, NY 11973-5000
www.bnl.gov

DISCLAIMER

Printed on recycled paper

Calibration and Testing of a Large-Area Fast-Neutron Directional Detector

Peter E. Vanier, *Member, IEEE*, Leon Forman, Istvan Dioszegi, Cynthia Salwen, and Vinita J. Ghosh

***Abstract*– We have developed a new directional fast-neutron detector based on double proton recoil in two separated planes of plastic scintillators with continuous position-sensitive readout in one of two dimensions. This method allows the energy spectrum of the neutrons to be measured by a combination of peak amplitude in the first plane and time of flight to the second plane. The planes are made up of 100-cm long, 10-cm high paddles with photomultipliers at both ends, so that the location of an event along the paddle can be estimated from the time delay between the optical pulses detected at the two ends. The direction of the scattered neutron can be estimated from the locations of two time-correlated events in the two planes, and the energy lost in the first scattering event can be estimated from the pulse amplitude in the first plane. The direction of the incident neutron can then be determined to lie on a cone whose angle is determined by the kinematic equations. The superposition of many such cones generates an image that indicates the presence of a localized source. Setting upper and lower limits on time of flight and energy allows discrimination between gamma rays, muons and neutrons. Monte Carlo simulations were performed to determine factors affecting the expected angular resolution and efficiency. These models show that this design has a lower energy limit for useful directional events at about 250 keV, because lower energy neutrons are likely to scatter more than once in the first plane.**

I. INTRODUCTION

WE have previously reported on the construction of an 8-element double-scatter neutron detector and demonstrated the principles of directional fast-neutron detection and neutron-gamma discrimination by time of flight [1,2]. In that prototype, the possible locations of scattering events were defined by 12.5-cm disk-shaped plastic scintillators, each attached to its own photomultiplier. There were only 4 pixels in each plane, giving a limited set of possible scattering angles, and large uncertainties in those angles. Also, the absolute efficiency was reduced by the unused spaces between the disks. Therefore, although that design could locate a point source at distances up to 9 m, it was unsatisfactory because it produced patchy images with non-uniform response and required long acquisition times. Similar results have been obtained by Mascarenhas and coworkers [3] using an 8-element in-line (rather than interleaved) design with liquid organic scintillators capable of pulse-shape discrimination.

In this paper, we report on the performance of a larger area (40 cm x 100 cm) double-scatter neutron detector with continuous readout of the position of an event in the horizontal direction (Fig. 1). There are four front and four back paddles stacked vertically, with a photomultiplier tube (PMT) at each end of each paddle. In this design, there are many possible scattering angles, and the area is closely tiled for optimum efficiency. There are some similarities to the Modular Neutron Array (MONA) detector [4] at Michigan State University, which was designed for high energy neutrons generated at an accelerator. Our system detects fission spectrum neutrons (1-5 MeV), is also modular, and can be easily expanded to 80 cm high or more by adding more paddles. The objective of the present application of this technique is to locate a source of fission neutrons at long stand-off distances. It is important to collect as many neutrons as possible in a short time, requiring large area, high sensitivity detectors. Plastic scintillators are available commercially in large areas at reasonable costs and are sensitive to gammas, neutrons and muons. We can distinguish different types of radiation by time-of-flight between two planes.

Fig. 1 Large area double-scatter fast neutron directional detector.

Manuscript received November 23, 2007.

P. E. Vanier, Cynthia Salwen, Istvan Dioszegi and Vinita Ghosh are with the Nonproliferation and National Security Department, Brookhaven National Laboratory, Upton, NY 11973, USA (telephone: 631-344-3535, e-mail: vanier@bnl.gov).

Leon Forman is with Ion Focus Technology, Miller Place, NY, USA and is a consultant to Brookhaven National Laboratory.

II. Principles of Operation

The scattering of neutrons in two layers of plastic scintillators is depicted in Fig. 2. The front layer thickness is 2 cm, giving about 25% probability of scattering a 2-MeV neutron. The back layer is 5 cm thick, with about 60% scattering probability. Assuming half the neutrons scattered in the first layer hit the second layer, the efficiency is expected to be roughly 0.25 x 0.6 x 0.5 = 7.5%. Some of these events will also be rejected by the discrimination hardware and software. The energy deposited by the recoiling proton in the front layer is measured by the geometric mean of the peak areas of the pulses recorded by the two PMTs, calibrated using the Compton edge for a ^{60}Co source. The calibration process includes a conversion from electron energy to proton energy based on an empirical scintillator response function [5]. The location of an event along any of the paddles is determined by the time delay between the light pulses arriving at the PMTs. The time of flight from the front plane to the back plane is used to determine the energy of the scattered neutron.

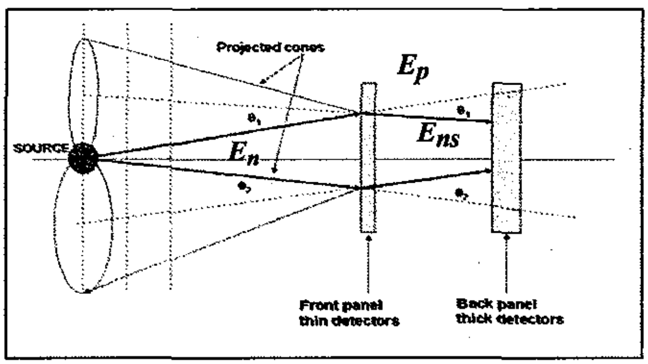

Fig. 2. Back projection of two double-scatter neutron events to locate a source.

The angle of scatter is related to the measured energies by the equations:

$$\tan^2\theta = E_p/E_{ns} \qquad \text{.................(1)}$$
$$E_n = E_p + E_{ns} \qquad \text{.................(2)}$$

where θ is the scattering angle, E_p is the energy of the first recoil proton, E_{ns} is the energy of the scattered neutron and E_n is the incident neutron energy.

At this time, only three front and three back paddles have been calibrated and tested, but the design includes a total of eight of each, which would give a total area of 8000 cm^2. The spacing between the front and back planes is adjustable between about 50 and 90 cm.

The signals from all channels are split between the inputs to a 1 Gs/s Acqiris digitizer and a set of NIM Constant Fraction Discriminators that provide logic inputs to the coincidence logic modules using 500 ns gates. The two pulses from each paddle are fed to an AND gate, generating a signal identifying the paddle involved. The front paddle logic signals are combined with OR gates, as are the back paddle logic signals. A trigger is generated by an AND gate combining front and back events. Whenever the free-running digitizer receives an event trigger, it transfers the data in all channels from the previous 500 ns to the controlling computer. A LabView™ controlling program is used to process the traces to determine the peak areas and relative timing of the leading edges. One data point is recorded per nanosecond per channel, and the leading edge time is determined by interpolation in units of 0.1 ns.

III. Calibration

The position sensing of the paddles using the time of arrival of the light pulses propagating in the plastic has been calibrated empirically using gamma sources moved along the surface of the scintillators in steps of 10 cm. Examples of the time distributions obtained from a ^{60}Co source are shown in Fig. 3. We estimate the full-width at half-maximum (fwhm) of these distributions to be 2.4 ns but their centroids can be determined much more precisely.

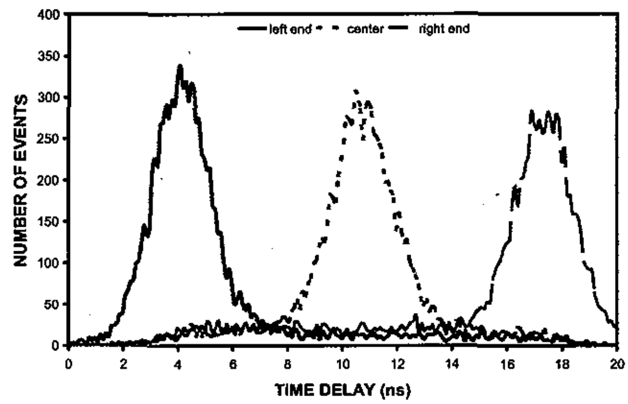

Fig. 3. Histograms of time delays between pulse leading edges at two ends of a paddle.

Calibration curves of mean time difference versus source position were obtained empirically for both front (thin) and back (thick) paddles using both ^{60}Co and ^{137}Cs sources. In the plots shown in Fig. 4, the slopes of the fitted lines correspond to a propagation velocity of light pulses in the plastic guides of 7.6 cm ns^{-1}. Thus the spatial resolution of the paddle is approximately 18 cm horizontally and 10 cm vertically.

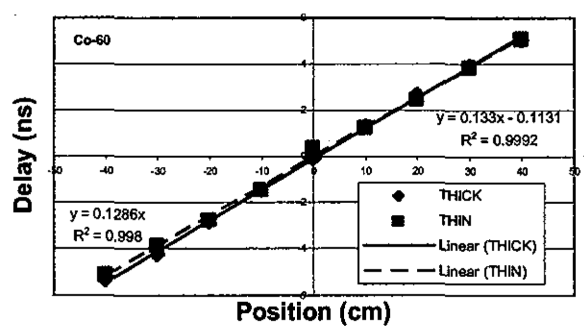

Fig. 4. Histograms of mean time differences between pulse leading edges at two ends of a paddle, measured at 10 cm intervals.

IV. Sorting Types of Events

The paddles are sensitive to Compton-scattered gamma-ray events, to muons making minimally ionizing charged-particle tracks, and to neutrons producing recoil-proton tracks. A number of possible coincidence events can occur involving a front paddle and a back paddle. These are illustrated in Figure 5, and can be listed as follows:

1. Compton scattered gammas
2. Muons from cosmic rays
3. Double-scattered neutrons
4. Associated particle γ in front, neutron in back layer
5. Associated particle γ in back, neutron in front layer
6. Neutron multiply scattered in front, then back
7. Accidental random gamma coincidences.

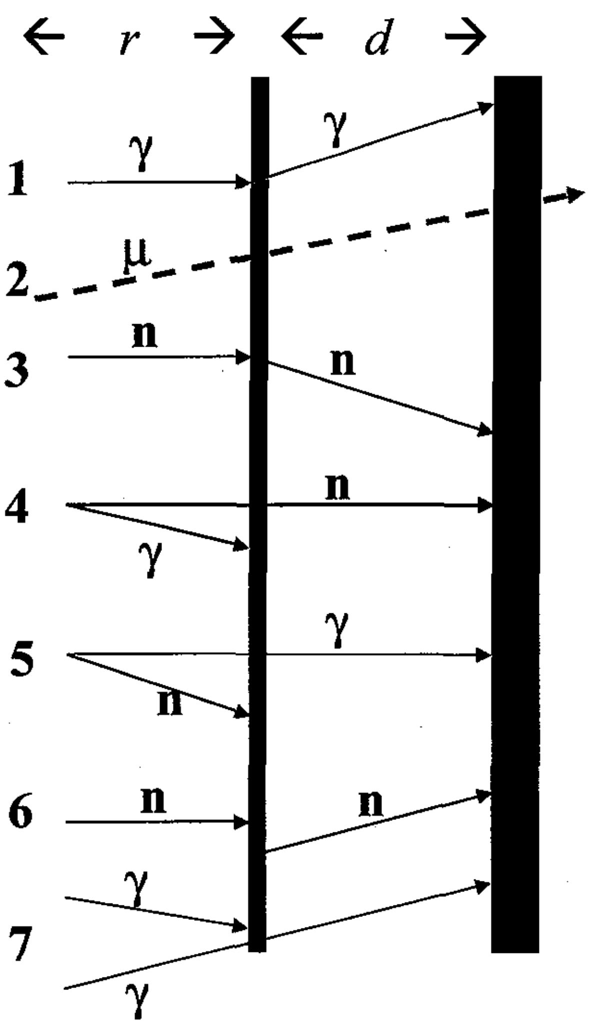

Fig. 5. Different types of coincidence events in the double-scatter fast neutron directional detector. Event type 3 is the neutron double scatter that we would like to analyze. Source to front layer range, r = 50-200 cm. Layer spacing, d= 50-86 cm.

The seven types of coincidence events are observed in our data, and can be sorted out by means of pulse amplitude and time of flight (see Fig. 6). Other experimenters [3] also use pulse shape discrimination to distinguish gamma rays from neutrons, which is possible when liquid organic scintillators are employed, but not with solid plastic.

The muon pulses are the largest in amplitude, since their tracks traverse the entire thickness of the paddles. They can be cut from the data using an upper amplitude limit. However, they are very useful during calibration because they produce a definite peak in the energy spectrum, whereas gamma rays produce only a Compton edge in plastic scintillators, and no photopeaks.

The Compton gamma rays can be removed from the data using a minimum time of flight such that only particles moving at velocities less than the speed of light are included.

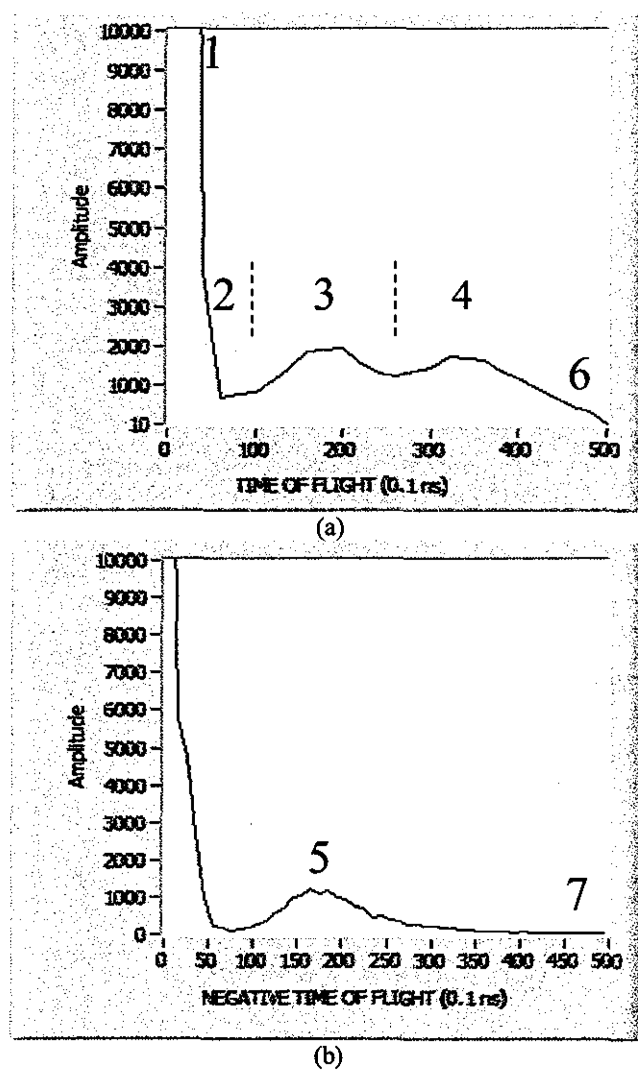

Fig. 6. TOF histograms for r=50 cm, d =50 cm. (a) Front layer triggered first, positive TOF. Type 3 events represent fission neutrons from Cf-252 traveling 50 cm in 15 - 25 ns. (b) Negative TOF means the back layer is triggered first by a gamma, as in processes 5 and 7.

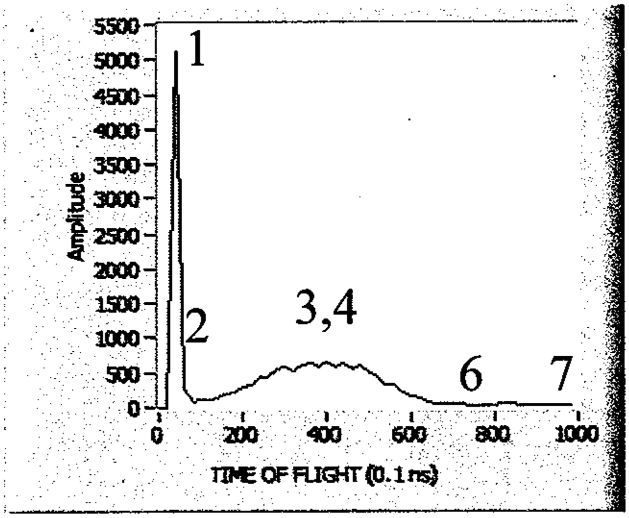

(a)

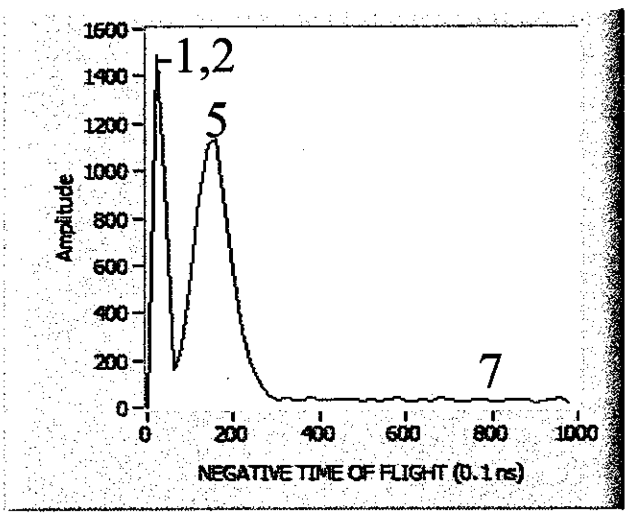

(b)

Fig. 7. TOF histograms for r=50 cm, d =86 cm. Processes 3 and 4 shift to longer time of flight, and merge. Process 5 stays the same.

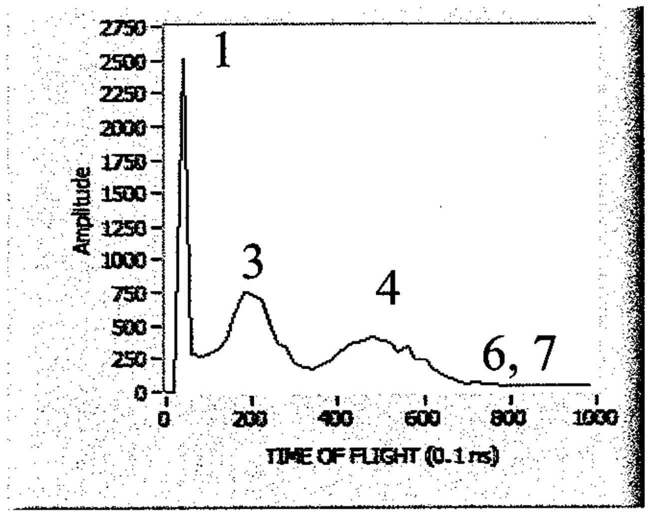

(a)

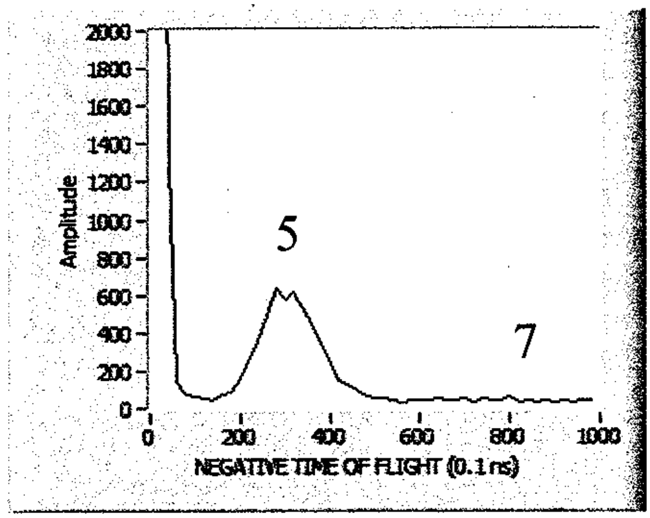

(b)

Fig. 8. TOF histograms for r=100 cm, d=50 cm. Processes 4 and 5 shift to longer times of flight.

The identification of features in Fig. 6 with processes in Fig. 5 can be confirmed by changing the separations r and d and observing the corresponding shifts in the features of the TOF histograms. In Fig. 7, data are presented for a wider layer spacing (86 cm) in which processes 3 and 4 are no longer resolved in TOF, but process 5 remains unchanged.

On the other hand, as the source range increases to 100 cm or more, with the layer spacing set at 50 cm, the peaks corresponding to processes 3 and 4 become more separated, and process 5 shifts to a longer "negative" time of flight (see Fig. 8). As the range is increased to longer distances, processes 4 and 5 are expected to become negligible, since they depend on two correlated particles emitted by the same fission event, the flux of each diminishing as $1/r^2$ and the combined process falling off as $1/r^4$.

In process 6, the incident neutron scatters more than once in the first layer (thereby losing its directional information). This is the most likely outcome for incident neutrons with energies below 0.5 MeV. Such events have longer TOFs and lower scattered energies than average. However, for neutron energies above 1 MeV, the chance of scattering more than once in the first layer diminishes, and the chance of a single scattering event increases. This is illustrated by MCNP calculations described in the next section.

Process 7 represents random accidental coincidences involving two gamma rays, not from the same fission event, that interact independently with the two layers. These events are equally likely to start with the front or the back detector. They are most easily seen in the flat region of the "negative" TOF histogram, where the rate is independent of the time delay, a consequence of a roughly constant background gamma count rate from natural radioactivity.

In the absence of a manmade source, the detector accumulates natural background, as shown in Fig. 9. These data show that, in the TOF region of interest, the background neutrons generated by cosmic rays are 3 times as numerous as the accidental gammas from the background. Consequently, even if gammas could be better rejected using pulse shape discrimination, the background neutrons would remain to interfere with the measurement. Ultimately, a weak manmade neutron source must be detected in the presence of background by means of its localized spatial signature. Both background neutrons and accidental gammas will appear to be fairly smooth and featureless, while a threat object should stand out as a bright spot. Note that in Fig. 9 (b) there is little evidence of double-scattered neutrons traveling in the reverse direction. The layer thicknesses of 2 cm in front and 5 cm in the back were chosen to optimize the forward double scattering process, and are not very efficient in the reverse direction.

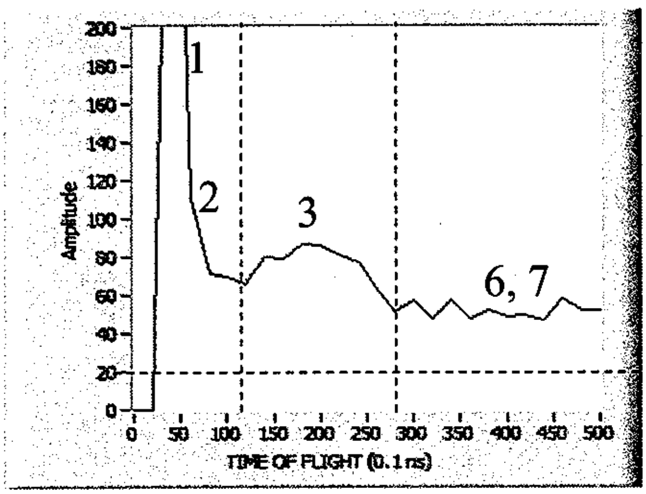

(a)

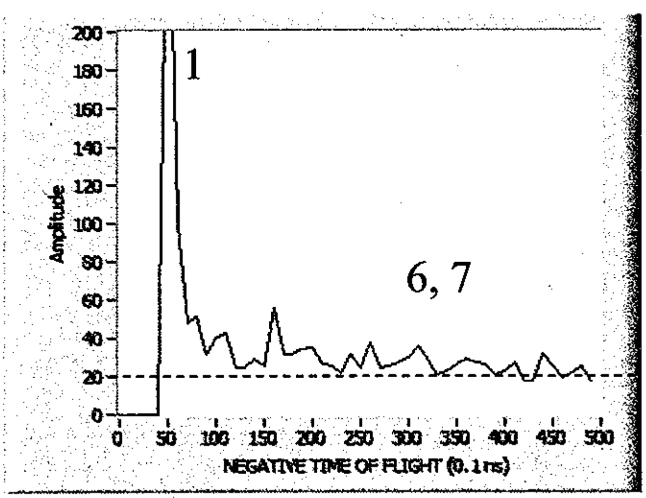

(b)

Fig. 9. TOF histogram for background measurements over 2 days (a) front paddle triggers first, (b) back paddle triggers first.

V. Monte Carlo Modeling

The double-scatter process was modeled using MCNPx to estimate the expected angular resolution and efficiency of the experimental configuration. This capability allows us to understand the underlying processes and to explore a variety of geometries without having to construct them. Figure 10 shows an example of a calculated result for the energy distribution of neutrons after scattering in the 2-cm front layer, starting with incident energy of 1 MeV. This plot shows that most scattered neutrons with energy less than about channel 5, corresponding to about 250 keV, undergo multiple scattering in the first layer and are therefore not useful for determining the source direction. On the other hand, scattered neutrons with energies greater than 0.5 MeV are more likely to have scattered only once in the first layer. This knowledge allows us to put an upper limit on the time of flight (or a minimum energy) of scattered neutrons used to plot the source direction.

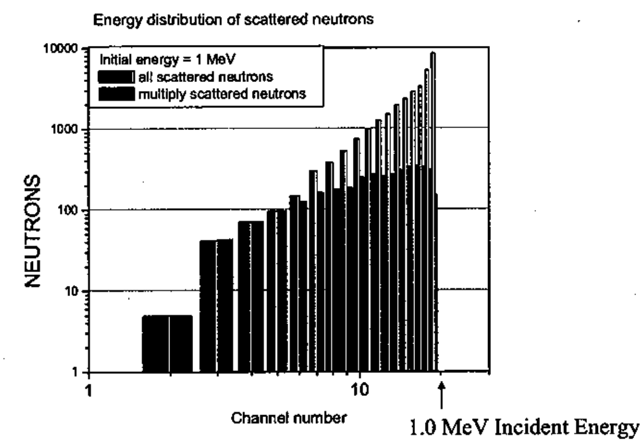

Fig. 10. Simulation of single and multiple scattering in front layer by MCNPx.

By keeping tallies on the individual neutron trajectories, calculating the angles of scatter, and back-projecting the cones of possible incident angles using estimates of the uncertainties in event position, we generated intensity plots to simulate the expected directionality of the detector. Example plots are shown in Figs. 11 and 12.

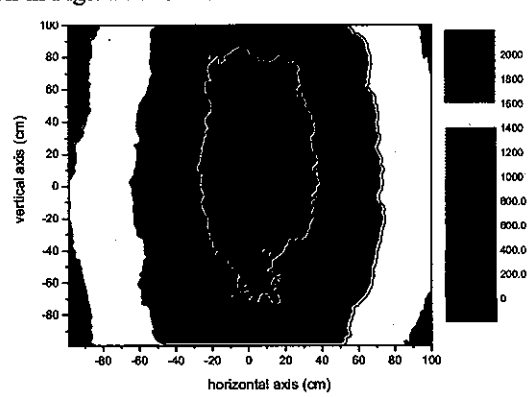

Fig. 11. Back projection of simulated scattering angles, assuming 10-cm spatial resolution in front and back planes. The projection plane is at $r = 10$ m, and the 2 m x 2 m projection plane has an angular field of view of ± 5.7°

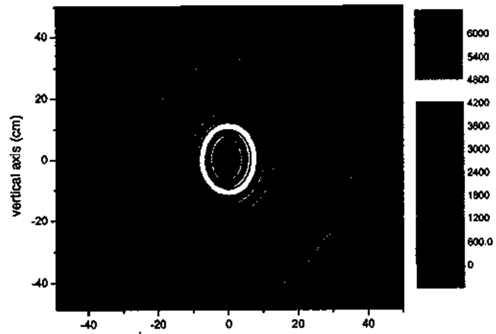

Fig. 12. Back projection of simulated scattering angles, assuming 1-cm spatial resolution in front and back planes. The projection plane is at $r = 10$ m, so the 1 m x 1 m projection plane has an angular field of view of $\pm 2.9°$.

These plots demonstrate that the precision of locating a target and also the contrast of the image are strongly affected by the spatial resolution of the detector elements. For neutrons with energy of 1 MeV incident on the front plane, the probability of a "good" event (in which a single scatter occurs in the front layer and at least one scatter occurs in the back layer) is estimated from the simulations to be about 1 %, and is expected to increase for higher energies. The fission spectrum for ^{252}Cf has a maximum at about 2 MeV, and the energy tail extends to more than 10 MeV. The efficiency of detecting fast neutrons with this device [6] should be ~6 %, which compares well with other methods, such as moderating and the neutrons with polyethylene and detecting them with ^{3}He gas ionization tubes.

VI. Experimental Images

Using 3 front panels and 3 back paddles (a total of 12 data channels, or 3000 cm^2 area) we obtained double-scatter data with neutrons from a ^{252}Cf source placed at various angles to the detector axis. The back-projection images created by simple addition of the ellipses from individual neutron events are shown in Fig. 13. A lower level threshold was applied to these images to eliminate the intensity due to parts of the ellipses that tended not to overlap. We recognize that there are more advanced image processing techniques that have been developed for Compton cameras, and these could be used in the future.

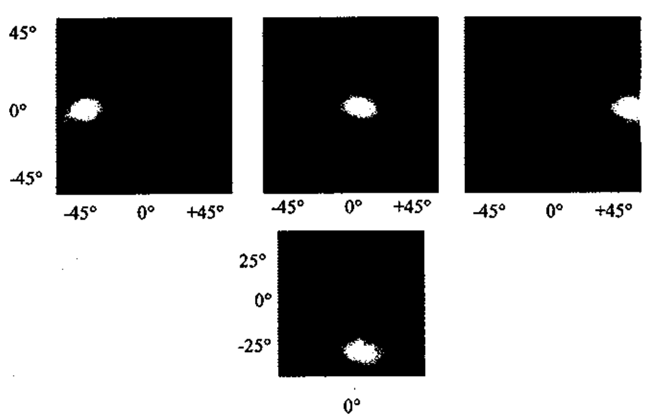

Fig. 13. Images of ^{252}Cf source produced by back-projection of experimentally determined cone angles using three pairs of paddles.

VII. Conclusions

We have demonstrated the operation of a paddle-based large-area double-scatter directional fast-neutron detector operating at present with an effective area of 3000 cm^2. The design allows a straightforward expansion to 8000 cm^2 or greater, which will reduce the time to detect and locate neutron source at longer stand-off distances. The angular resolution is affected both by the spatial resolution of the paddles and by the uncertainty of the peak area measurement. There is a potential to improve both of these in the future. As the area gets larger, the spacing between the planes can be increased without a great loss of efficiency, but improving the precision of the TOF and the scatter angle. The maximum range at which a given source can be detected will depend on the effectiveness of the spatial filtering to extract a point source from the relatively smooth, isotropic background of cosmogenic neutrons. The fast component of these neutrons dominates over the accidental coincidences generated by background gamma rays. The length of time required to acquire statistically significant data will depend on the area, the efficiency, the angular resolution and the image processing algorithms. Modeling can provide insights into the physical processes and trends, but may not include all sources of error that exist in the empirical data.

VIII. Acknowledgements

We are grateful to Sara Pozzi of ORNL for performing independent simulations of the double scatter configuration, confirming our estimates of efficiency.

This work was supported by U.S. Department of Energy, Office of Nonproliferation Research and Development.

This manuscript has been authored by Brookhaven Science Associates, LLC under Contract No. DE-AC02-98CH1-886 with the U.S. Department of Energy. The United States Government retains, and the publisher, by accepting the article for publication, acknowledges, a world-wide license to publish or reproduce the published form of this manuscript, or allow others to do so, for the United States Government purposes.

IX. References

[1] Peter E. Vanier and Leon Forman, "An 8-element fast-neutron double-scatter directional detector", Proceedings of the SPIE – Hard X-ray and Gamma-ray Detector Physics VII, 5923-8, San Diego, CA, August, 2005.

[2] Peter E. Vanier and Leon Forman, "Demonstration of a Directional Fast Neutron Detector", Conference Record of IEEE Nuclear Science Symposium, Puerto Rico, 2005.

[3] N. Mascarenhas, J. Brennan, J. Lund, U. Bravar, and J. Ryan, "Development of neutron scatter camera for fission neutrons", Conference Record of IEEE Nuclear Science Symposium, San Diego, CA, 2006.

[4] Modular Neutron Array (MONA) web page, Michigan State University, http://www.cord.edu/dept/physics/mona/.

[5] R.A. Cecil, B.D. Anderson and R. Madey, "Improved predictions of neutron detection efficiency for hydrocarbon scintillators from 1 MeV to about 300 MeV", Nucl. Inst. & Meth., 161, pp. 439-447, 1979.

[6] Independent MCNP-PoliMi simulations of this configuration performed at Oak Ridge National Laboratory arrived at similar conclusions. Sara Pozzi, private communication.